

Nonlinear Switching of Optical Pulses in Fiber Bragg Gratings

Hojoon Lee, *Member, IEEE*, and Govind P. Agrawal, *Fellow, IEEE*

Abstract—We study numerically the nonlinear switching characteristics of optical pulses transmitted through fiber Bragg gratings. We consider both the uniform and phase-shifted gratings and compare their performance as a nonlinear switch. The nonlinear coupled-mode equations were solved numerically to obtain the pulse-switching characteristics. The steady-state behavior known to occur for continuous-wave optical beams is realized only for pulses wider than 10 ns with long tails. For pulsewidths in the range 0.1–1 ns, the use of phase-shifted gratings reduces the switching threshold, but the on-off contrast is generally better for uniform gratings. We also quantify the effects of rise and fall times associated with an optical pulse on nonlinear switching by considering the Gaussian pulses with smooth tails and nearly rectangular pulses with sharp leading and trailing edges.

Index Terms—Bragg gratings, fiber gratings, nonlinear optics, optical switches, periodic structures.

I. INTRODUCTION

FIBER Bragg gratings (FBGs) are attractive for their applications in the fields of optical communication systems and optical fiber sensors [1]. Although most applications have focused on the linear properties of FBGs, Bragg gratings also offer the potential of nonlinear switching, a phenomenon that has attracted considerable attention since 1979 [2]–[18]. In a 1995 experiment, intense optical pulses were propagated through a FBG (approximately 1 cm in length) at frequencies inside the photonic bandgap [7]. Although the intensity-dependent transmission was measured, it was not possible to observe the propagation effects as the pulses were much longer than the grating. The propagation of Bragg-grating solitons in long and uniform FBGs was first observed in a 1996 experiment [19], in which soliton-like pulses were observed to propagate at $\sim 75\%$ of the speed expected in the absence of the FBG. Similar effects occur in superstructure Bragg gratings, as discussed in [20].

The Bragg grating solitons form in FBGs through a balance between the strong grating dispersion and the third-order optical nonlinearity and propagate at velocities substantially below the speed of light in a bare fiber [21]. A numerical analysis shows that these solitons are well described by the solitary-wave solutions of the nonlinear coupled-mode equations [22]. The nonlinear reflection of optical pulses in a chirped FBG is also of interest [23]. It was found that for incident pulse intensities

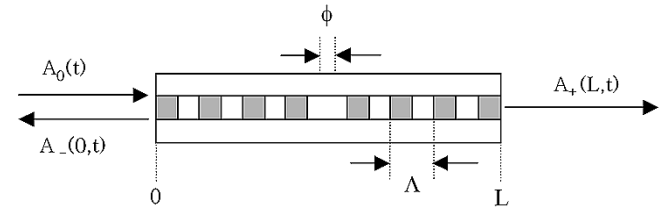


Fig. 1. Schematic of a phase-shifted FBG. The notation used in the paper is also illustrated.

in the regime suitable for the formation of fundamental solitons in transmission, pulse pairs are formed in reflection. The pulse-pair formation is associated with the strong fields produced as the pulse reflects from a chirped FBG.

Quasi-continuous-wave (CW) nonlinear switching within the bandgap of a FBG was observed in 1998 [10]. As many as five gap solitons of 100–500-ps duration were generated from a 2-ns pulse at a launched peak intensity of 27 GW/cm^2 . A corresponding increase in the transmission from 3% to 40% of the incident pulse energy was observed. In another experiment [12], all optical nonlinear switching in a 20-cm-long FBG led to a 20-dB increase in the transmissivity. All of these experiments require high peak intensities for nonlinear switching. One way to reduce the input intensity is to use a phase-shifted FBG. The theory of phase-shifted DFB structures in the CW regime developed in 1995 [4] shows not only low switching intensities, but also the possibility of frequency-controlled all-optical switching. One would expect these useful features to survive when short optical pulses are used in place of a CW beam. In this paper, we investigate the switching characteristics of optical pulses in uniform and phase-shifted FBGs and compare them with the CW case. We show that the results depend on the pulse shape by using Gaussian and raised-cosine pulses. We find that the switching threshold can be reduced significantly by using phase-shifted FBGs, provided the pulse shape is chosen judiciously.

II. THEORY

Fig. 1 shows a phase-shifted FBG schematically. The refractive index varies along the grating length periodically except for a phase-shift occurring in the middle of the grating. The index variation can be written as

$$n(z) = \bar{n} + n_1(z) \cdot \cos \left[\frac{2\pi}{\Lambda} z + \phi(z) \right] + n_2 |E(z)|^2 \quad (1)$$

where $E(z)$ is the electric field, \bar{n} is the average refractive index change of the fiber mode, $n_1(z)$ is the amplitude of periodic index change, n_2 is the nonlinear Kerr coefficient, Λ is the Bragg

Manuscript received September 19, 2002; revised October 30, 2002.

H. Lee is with the Institute of Optics, University of Rochester, Rochester, NY 14627 USA and also with the Department of Information and Communication Engineering, Hoseo University, Asan 336-795, Republic of Korea (e-mail: hojoon@office.hoseo.ac.kr).

G. P. Agrawal is with the Institute of Optics, University of Rochester, Rochester, NY 14627 USA.

Digital Object Identifier 10.1109/JQE.2002.808165

period, and $\phi(z)$ describes the phase shift. The same form can be used for chirped fiber gratings by making Λz -dependent. The electric field inside the grating can be written as

$$E(z, t) = [A_+(z, t) \exp(ik_B z) + A_-(z, t) \times \exp(-ik_B z)] \exp(-i\omega_0 t) \quad (2)$$

where $k_B = \pi/\Lambda$ is the Bragg wave number, A_+ and A_- are the envelope functions of the forward and backward-traveling wave, both of which are assumed to be slowly varying in space and time, ω_0 is the carrier frequency at which the pulse spectrum is initially centered, and $k = \bar{n}\omega_0/c$ is the propagation constant. The detuning parameter is defined as

$$\delta = k - k_B. \quad (3)$$

To describe nonlinear pulse propagation in FBGs, we use the nonlinear coupled-mode equations that are valid only for wavelengths close to the Bragg wavelength. Using (1) and (2) in the Maxwell equations, one obtains the following set of nonlinear coupled-mode equations [24]:

$$+i \frac{\partial A_+}{\partial z} + i \frac{1}{v_g} \frac{\partial A_+}{\partial t} + \delta A_+ + \kappa A_- + \Gamma |A_+|^2 A_+ + 2\Gamma |A_-|^2 A_+ = 0 \quad (4)$$

$$-i \frac{\partial A_-}{\partial z} + i \frac{1}{v_g} \frac{\partial A_-}{\partial t} + \delta A_- + \kappa^* A_+ + \Gamma |A_-|^2 A_- + 2\Gamma |A_+|^2 A_- = 0 \quad (5)$$

where $v_g = c/n_g$, n_g is the group index, and the linear coupling coefficient κ and the nonlinear parameter Γ are defined as

$$\kappa(z) = \frac{\pi n_1(z)}{\lambda_B} \exp[i\phi(z)], \quad \Gamma = \frac{2\pi}{\lambda_B} n_2 \quad (6)$$

where $\lambda_B = 2\bar{n}\Lambda$ is the Bragg wavelength and $\lambda = \omega_0/2\pi c$ is the carrier wavelength. The units of A_{\pm} are chosen such that $|A_{\pm}|^2$ represents intensity (W/m^2).

In general, the nonlinear coupled mode equations should be solved numerically for studying the nonlinear effects. We use the finite-difference method developed in [25]. The method uses the characteristics associated with (4) and (5) and solves them on a two-dimensional grid using an implicit fourth-order Runge-Kutta scheme, while combining the results at the grid points. In this method, the number of sections into which the grating is divided depends on the number of grid points in the time direction. Since the use of characteristics converts the two partial differential equations into two ordinary differential equations, one can apply the methods developed for solving ordinary differential equations. In the geometry of Fig. 1, a single pulse with the amplitude $A_0(t)$ is incident on the left end of the grating located at $z = 0$. The boundary conditions in this case become $A_+(0, t) = A_0(t)$, $A_-(L, t) = 0$, $A_+(z, 0) = 0$, and $A_-(z, 0) = 0$, where L is the grating length. In the following numerical simulations, we consider a fiber grating with the Bragg wavelength $\lambda_B = 1.55 \mu\text{m}$ and use $\bar{n} = 1.46$ and $n_2 = 2.6 \times 10^{-20} \text{ m}^2/\text{W}$ for the average index. The input intensities are given in units of gigawatts per square centimeter (GW/cm^2). The launched power can be obtained by multiplying them by the effective core area of the fiber. Switching power can be reduced using highly nonlinear fiber with larger n_2 values.

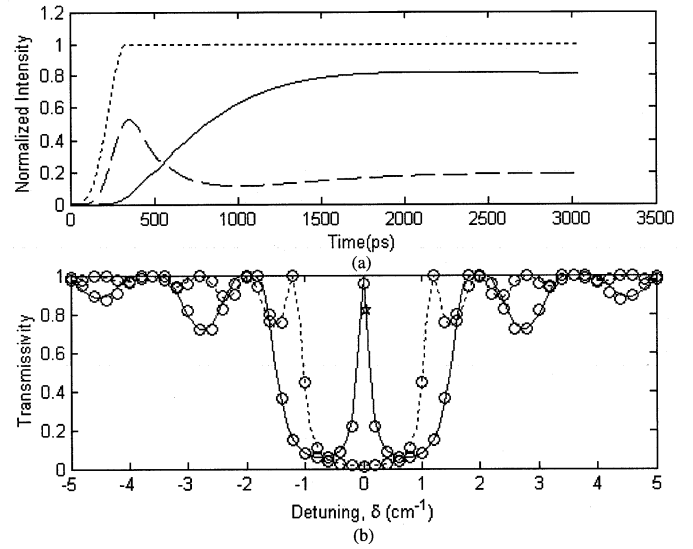


Fig. 2. (a) Transmitted (solid) and reflected (dashed) intensities when the input intensity (dotted) is increased rapidly to a final steady-state value. The final values after 3 ns agree with the CW Theory. (b) Steady-state transmission spectrum for two different phase shifts obtained using coupled-mode equation (circles) and CW matrix method (solid curves).

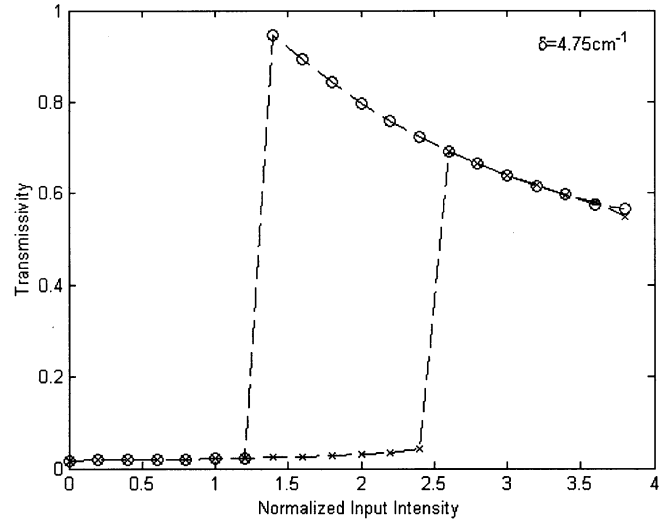


Fig. 3. Bistability characteristics obtained for very long pulse cases for a uniform grating ($\phi = 0$) using $\kappa = 5 \text{ cm}^{-1}$, $L = 1 \text{ cm}$, $\delta = 4.75 \text{ cm}^{-1}$. Crosses and circles show the off and on branches with hysteresis.

III. QUASI-CW SWITCHING CHARACTERISTICS

Before focusing on the phenomenon of nonlinear switching, we consider the linear case and solve the coupled-mode equations after setting $\Gamma = 0$. To show the effect of phase shift ϕ on the transmission spectrum of a FBG, we consider the CW limit by using an input field whose intensity rises quickly (rise time $\sim 100 \text{ ps}$) and then settles down to a constant value (similar to a step function). The dotted line in Fig. 2(a) shows the input intensity profile. The solid and dashed lines show, respectively, the transmitted and reflected intensities for such an input when the signal wavelength almost coincides with the Bragg wavelength ($\delta = 0.005 \text{ cm}^{-1}$) and the grating has a π phase shift. A FBG with a coupling coefficient $\kappa = 0.8 \text{ cm}^{-1}$ and a length of 3.5 cm

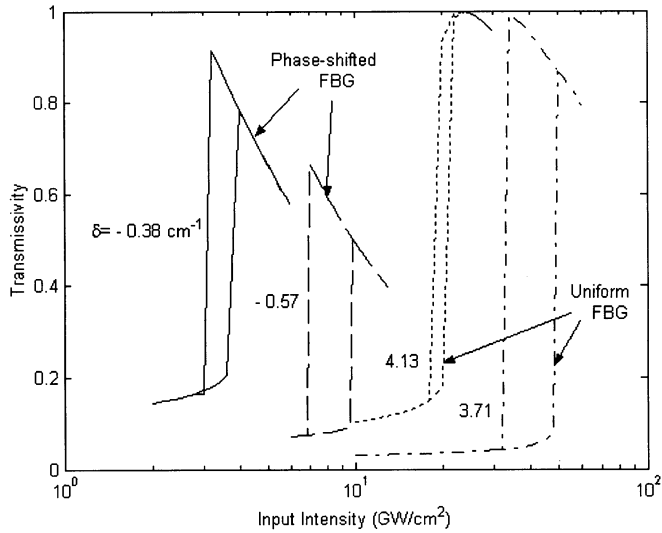


Fig. 4. Bistable features of phase-shifted gratings ($\phi = \pi$) for four choices of detuning.

was used. In this case, the steady state can be reached after 3 ns, as seen in Fig. 2(a). The initial delay and the raised-cosine function used for the leading edge are chosen carefully to avoid the initial shock that may occur with a mismatch of the initial and front-end boundary conditions at the input ($z = 0, t = 0$). The rise time of the transmission curve depends on the detuning parameter and is relatively large near the Bragg wavelength, as shown in Fig. 2(a).

Fig. 2(b) shows the CW transmission spectrum of phase-shifted FBGs by plotting the steady-state transmissivity obtained after 3 ns as a function of δ for $\phi = 0$ and π . The results obtained using the coupled-mode equations are shown with circles [the star corresponds to the case of Fig. 2(a)]. Dotted ($\phi = 0$) and solid curves ($\phi = \pi$) show the results obtained with the matrix method that is used commonly in the CW case. As seen in Fig. 2(b), the agreement between the two methods is excellent. As is well known [4], a phase shift opens a transmission peak within the stopband of an otherwise uniform grating, and the location of the peak depends on the amount of phase shift. The peak is located in the middle of the bandgap for $\phi = \pi$.

We next consider the case of a nonlinear grating. Again, we solve the nonlinear coupled-mode equation using the input with a sharp rising edge similar to that shown in Fig. 2(a). In the nonlinear case, the steady state was reached only after 6 ns. Because the nonlinear regime exhibits bistability, two different step functions were used to obtain the CW bistable characteristics shown in Fig. 3 for a uniform FBG with $\kappa = 5 \text{ cm}^{-1}$, $L = 1 \text{ cm}$, $\delta = 4.75 \text{ cm}^{-1}$, and $\phi = 0$. The lower branch was obtained using a step function with a rising edge while the upper branch required an opposite step function whose value falls from 1 to 0 with a fall time of about 200 ps. The results of Fig. 3 agree with the analytical prediction of [24] except that numerical method cannot reproduce the middle “unstable” branch of the S-shaped bistability curve.

Nonlinear switching characteristics for uniform and phase-shifted FBGs are compared in Fig. 4. The two bistability curves

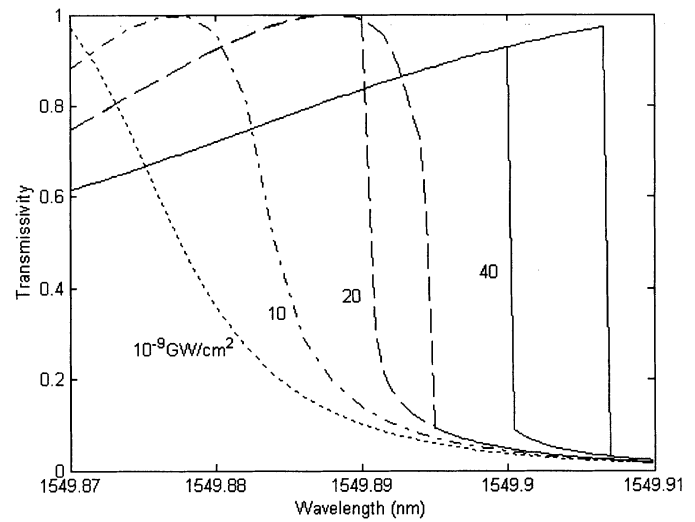


Fig. 5. Spectral bistability for uniform gratings at input intensity levels. At $I = 1 \text{ W/cm}^2$, the nonlinear effects are negligible and bistability does not occur.

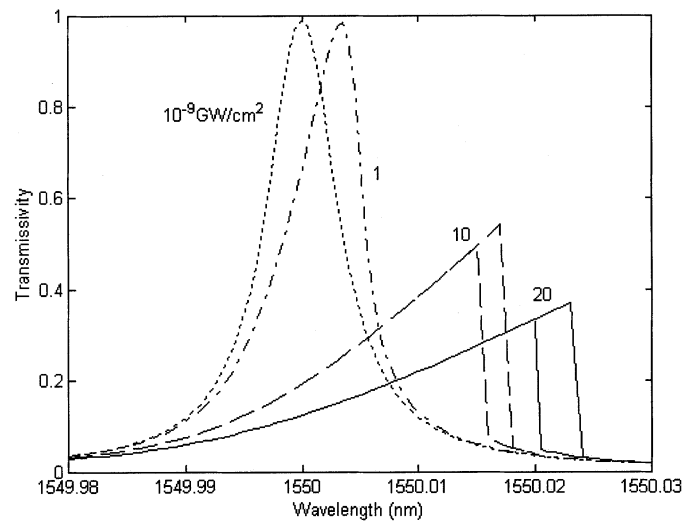


Fig. 6. Spectral bistability for phase-shifted gratings ($\phi = \pi$) at the same four intensity levels for near $\delta = 0$.

on the left side are for a phase-shifted FBG while the other two on the right side are for a uniform FBG. The switching intensity of uniform FBGs is more than five times larger than that of phase-shifted FBGs. This reduction was predicted by Radic *et al.* in 1995 using a CW theory. Note, however, that the on-off ratio of nonlinear switching is better for uniform FBGs.

Optical switching can also occur at a constant input intensity provided the wavelength is changed by changing the detuning parameter. Figs. 5 and 6 compare the switching characteristic in the case of uniform and phase-shifted FBGs, respectively. A grating with $\kappa = 4 \text{ cm}^{-1}$ and $L = 1 \text{ cm}$ is used in these simulations. In both the uniform and phase-shifted cases, transmissivity can be switched from low to high values by changing the input wavelength by a relatively small amount. The required change in the input frequency is $< 1 \text{ GHz}$. Such a small change can be realized by temperature tuning when a semiconductor

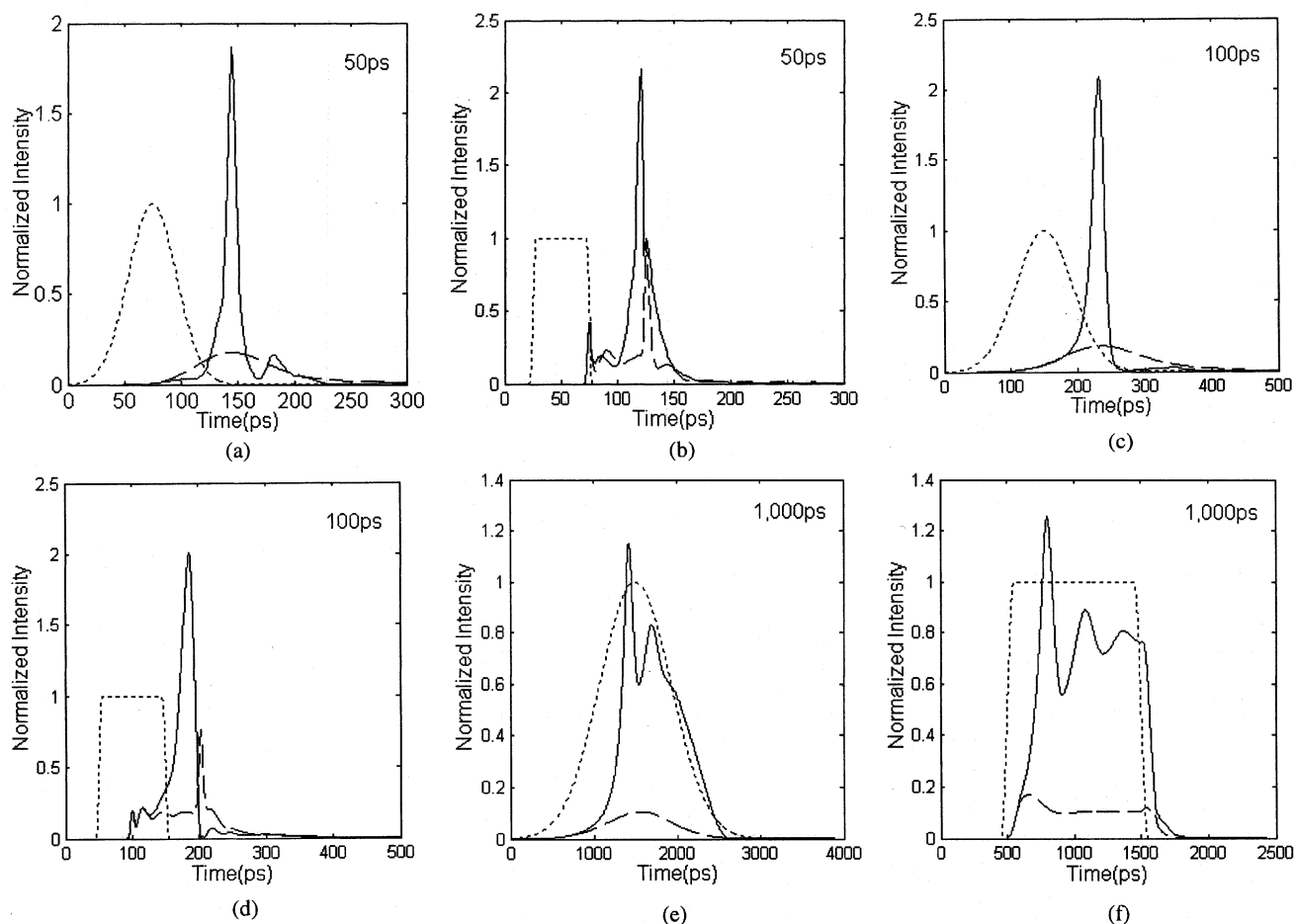


Fig. 7. Transmitted pulse shape in the on (solid) and off (dashed) states for Gaussian (left column) and square-shaped (right column) input pulses shown by dotted curves in the case of a uniform FBG. Pulswidths are 50, 100, and 1000 ps.

laser is used. In the case of phase-shifted gratings, the input frequency needs to be changed by < 300 MHz. Such a small frequency shift can be realized using an acousto-optic modulator. The on-off contrast is again smaller in the case of phase-shifted gratings.

IV. SHORT-PULSE SWITCHING CHARACTERISTICS

We now consider how the switching characteristics are affected as the pulswidth is reduced from tens of nanoseconds to below 100 ps. The shape of the transmitted pulses can change dramatically from that of the input pulse, especially when pulses are short. Figs. 7 and 8 show the transmitted pulse shapes in the on (solid curves) and off (dashed curves) states for a variety of input pulses in the case of uniform and phase-shifted gratings, respectively. In both cases, the left and right columns are for Gaussian and square-shaped pulses (dotted curves), respectively, and the pulswidth is chosen in the 50–1000 ps range.

In the case of a uniform grating (Fig. 7), the 1-ns-long pulse exhibits quasi-CW characteristics except for the relaxation oscillations seen in the bottom traces of Fig. 7. These oscillations can be attributed to the phenomenon of modulation instability. For pulses shorter than the round-trip time within the grating, the transmitted pulse is significantly compressed. In fact, the

pulse has features similar to those associated with slow-moving Bragg-grating solitons.

In the case of phase-shifted FBGs shown in Fig. 8, the switching behavior is quite different compared with the uniform-grating case. For broad 1-ns pulses, we observe much less splitting, an indication that modulation instability is not playing a significant role. For shorter pulses, the transmitted pulse is much broader and much less intense than that in the uniform-grating case.

Bistable switching characteristic for short pulses are compared with the CW case in Fig. 9. Dashed curves show the case of a Gaussian-shape input pulse, while the solid curves correspond to a pulse whose shape is nearly rectangular with sharp leading and trailing edges. Pulswidths are 1000 and 100 ps [full-width at half maximum (FWHM)] in Fig. 9(a) and (b), respectively. In all cases, a phase-shifted FBG needs much lower switching intensity compared with the case of a uniform grating. However, pulswidth plays a major role, as is apparent from Figs. 7 and 8. In the case of 1-ns-wide pulses, switching threshold is almost the same as the CW case because the pulse bandwidth of 1 GHz is small enough for switching to occur. However, switching becomes much more gradual as the pulswidth decreases and its bandwidth increases. Note also that square-shaped pulses need a lower switching intensity compared with Gaussian pulses. This can be understood by

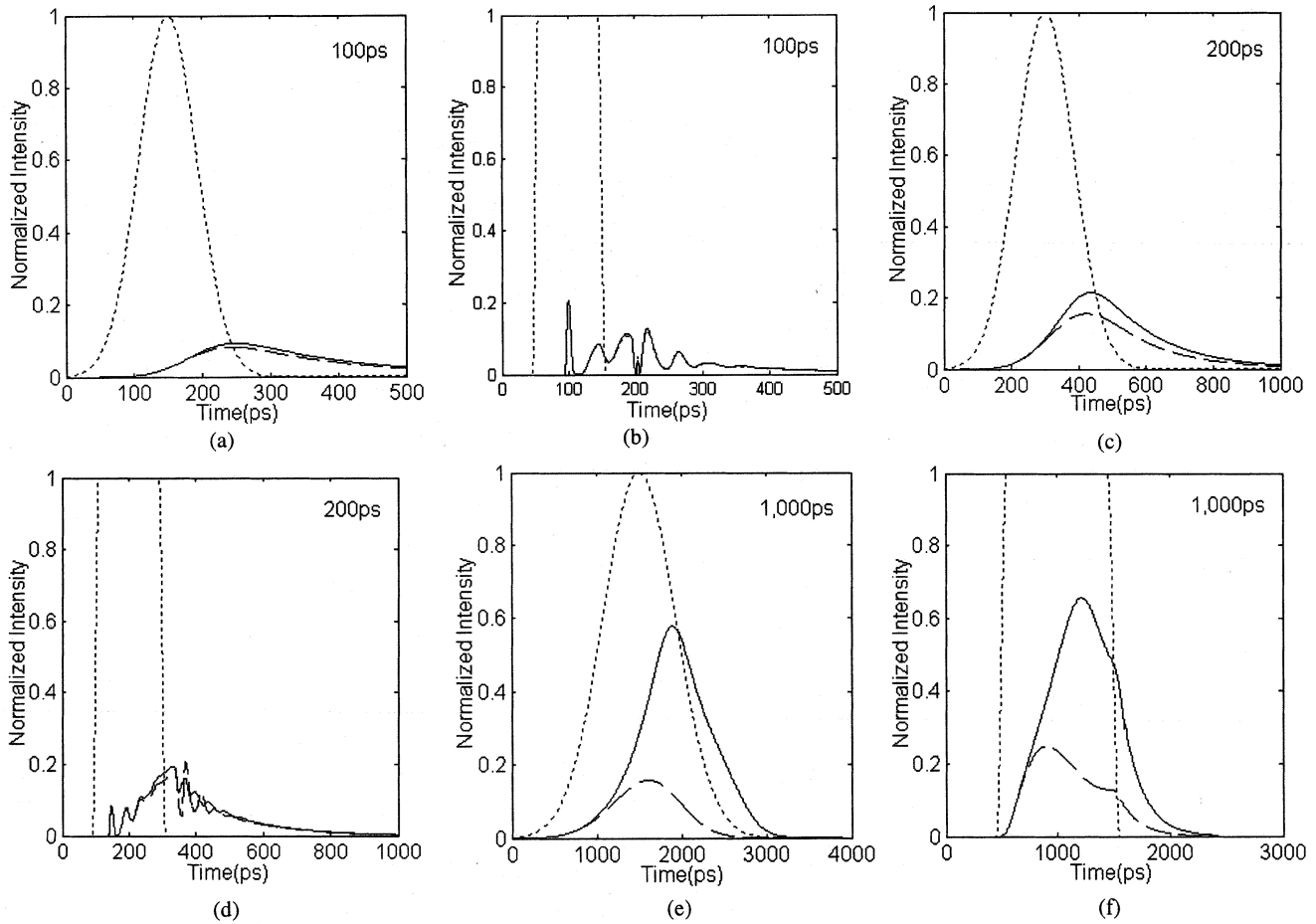


Fig. 8. Same as in Fig. 7 except that a phase-shifted grating is used and pulsewidths are 100, 200, and 1000 ps.

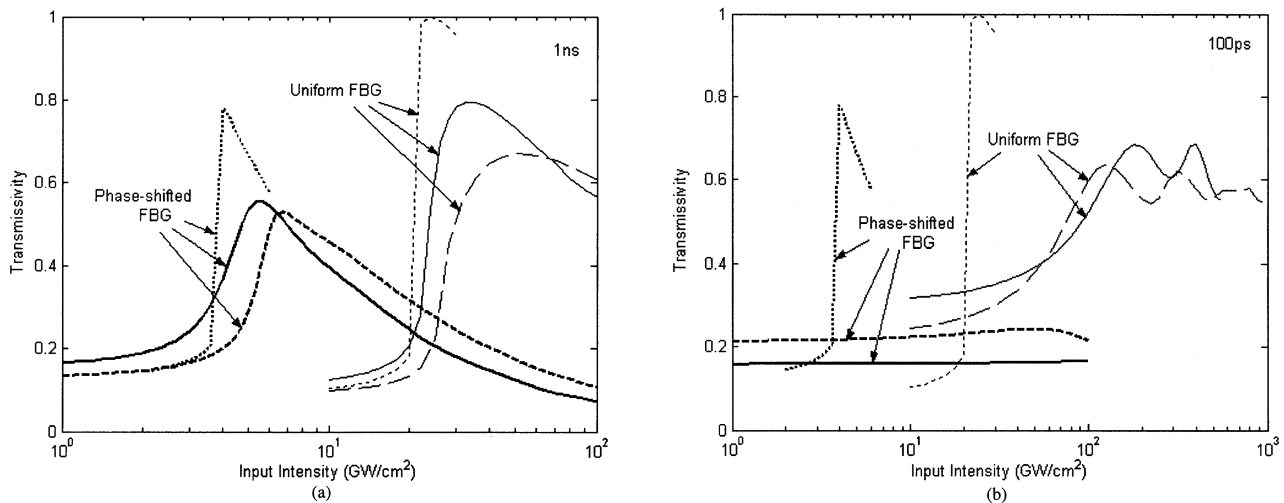


Fig. 9. Comparison of switching characteristics for uniform and phase-shifted gratings. Dotted, solid, and dashed curves show the CW, square-shaped, and Gaussian pulse cases, respectively. (a) Pulsewidth of 1 ns. (b) Pulsewidth of 100 ps.

noting that the switching depends mainly on the peak intensity of the pulse, but not on its bandwidth as long as the pulse is wider than 500 ps.

The switching depends on the pulse bandwidth in the case of short pulses shown in Fig. 9(b). The pulsewidth of 100 ps is too short to couple the forward- and backward-propagating waves

effectively inside a phase-shifted FBG of 1-cm length (transit time ~ 50 ps). In the case of a uniform FBG, the switching behavior can be observed even for short pulses, but at high intensities. In fact, as seen in Fig. 7, a gap soliton is formed in the on-state. Notice that as the pulsewidth decreases, switching becomes much more gradual. This can be explained by noting

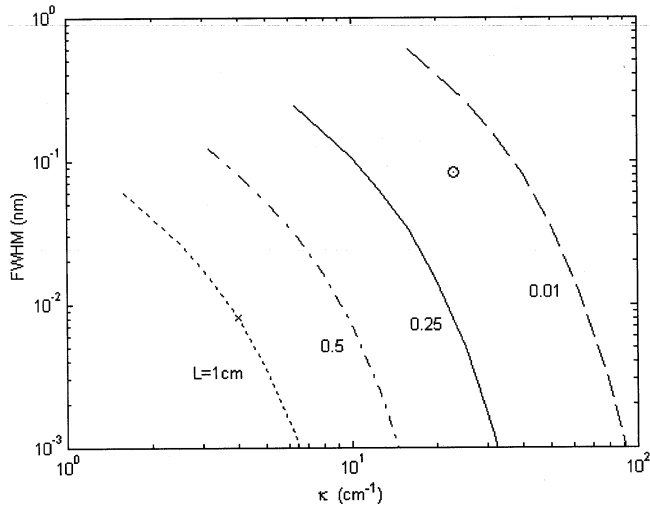


Fig. 10. FWHM of center passband for the phase-shifted FBG as a function of coupling coefficient for different grating lengths.

that the switching characteristics of a short pulse with many frequency components are averaged over the entire pulse spectrum.

However, in the case of a phase-shifted FBG, no change of transmission is observed with changes in the input intensity (see Fig. 8). The bandwidth of the passband for a phase-shifted FBG is important for switching a pulsed signal. Because the FWHM of this passband is about 1 GHz in our simulations, a 100-ps pulse with a bandwidth ~ 5 GHz cannot pass through it. However, in the case of a uniform FBG, switching is generated at the left edge of the bandgap, and the bandwidth of the uniform FBG is normally wider than that of the signal.

V. DESIGN OPTIMIZATION FOR PHASE-SHIFTED GRATINGS

One can design a phase-shifted FBG whose transmission passband is wide enough for 100-ps pulses. The transmissivity of a phase-shifted FBG within the central passband can be calculated analytically and is given by

$$T = \left[\frac{4\delta^2\kappa^2 \sinh^4 \left[(\kappa^2 - \delta^2)^{1/2} \frac{L}{2} \right]}{(\kappa^2 - \delta^2)^2} + 1 \right]^{-1}. \quad (7)$$

The spectral bandwidth for given values of κ and L is obtained by finding δ where the transmissivity drops to 50%. This occurs when δ is the solution of

$$4\delta^2\kappa^2 \sinh^4 \left[(\kappa^2 - \delta^2)^{1/2} \frac{L}{2} \right] = (\kappa^2 - \delta^2)^2. \quad (8)$$

Fig. 10 shows the FWHM as a function of the coupling coefficient κ for four different lengths of the FBG. As κ decreases for a given length of grating, the FWHM increases but the entire of bandgap shrinks and eventually the grating become useless. Typically, κL should exceed 2. The cross corresponds to the

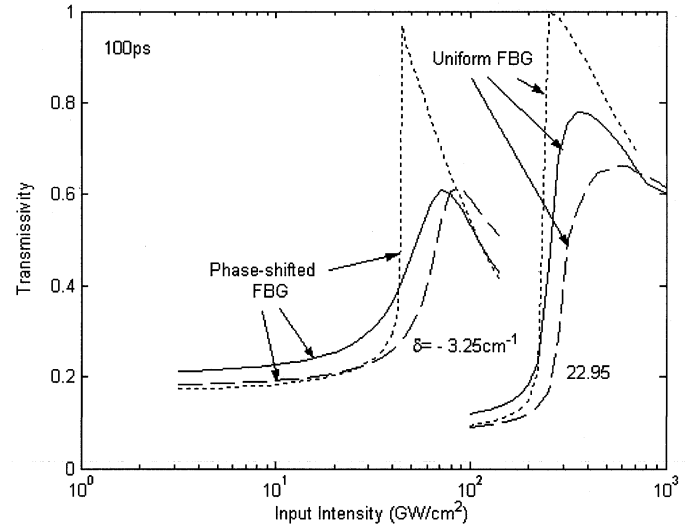


Fig. 11. Comparison of switching characteristics for uniform and phase-shifted gratings. Curves are shown for the CW (dotted curves), square shaped (solid curves), and Gaussian pulse (dashed curves). The grating parameters are $\kappa = 23 \text{ cm}^{-1}$ and $L = 0.15 \text{ cm}$.

phase-shifted grating used for Fig. 9(b). The passband FWHM is only ~ 1 GHz in this case. The circle shows a design choice for which the bandwidth exceeds 10 GHz. For this grating, $\kappa = 23 \text{ cm}^{-1}$, $L = 0.15 \text{ cm}$, and $\kappa L = 3.45$.

Fig. 11 shows the switching characteristics for this grating using pulses of 100-ps width. In the case of a phase-shifted grating, we can observe that the switching characteristics are comparable to the uniform FBG case but the switching intensity is lower by a factor of five. Note that the square shape has low-intensity switching characteristics for both of FBGs. Switched pulse shapes are shown in Fig. 12. The transmitted pulse for a phase-shifted FBG looks Gaussian. In contrast, oscillations are observed for a uniform FBG. We conclude that pulses as short as 100 ps can be used for nonlinear switching, if the grating parameters are chosen judiciously.

VI. CONCLUSIONS

In this paper, we have compared the switching characteristics of uniform and phase-shifted FBGs when optical pulses are sent through the grating. The nonlinear coupled-mode equations were solved numerically for pulsewidths ranging from 50 ps to 10 ns or more. For very long pulses (width > 10 ns), the switching behavior is similar to the quasi-CW case. For pulsewidths in the range 0.5–1 ns, phase-shifted gratings offer better switching characteristics. For pulses shorter than 500 ps, the phase-shifted FBGs need to be designed with values of $\kappa > 10 \text{ cm}^{-1}$ while keeping $\kappa L \approx 3$ so that the central transmission peak is wide enough for the entire pulse spectrum. In general, the use of phase-shifted FBGs reduces the switching intensity levels but the on-off contrast is generally better for uniform gratings.

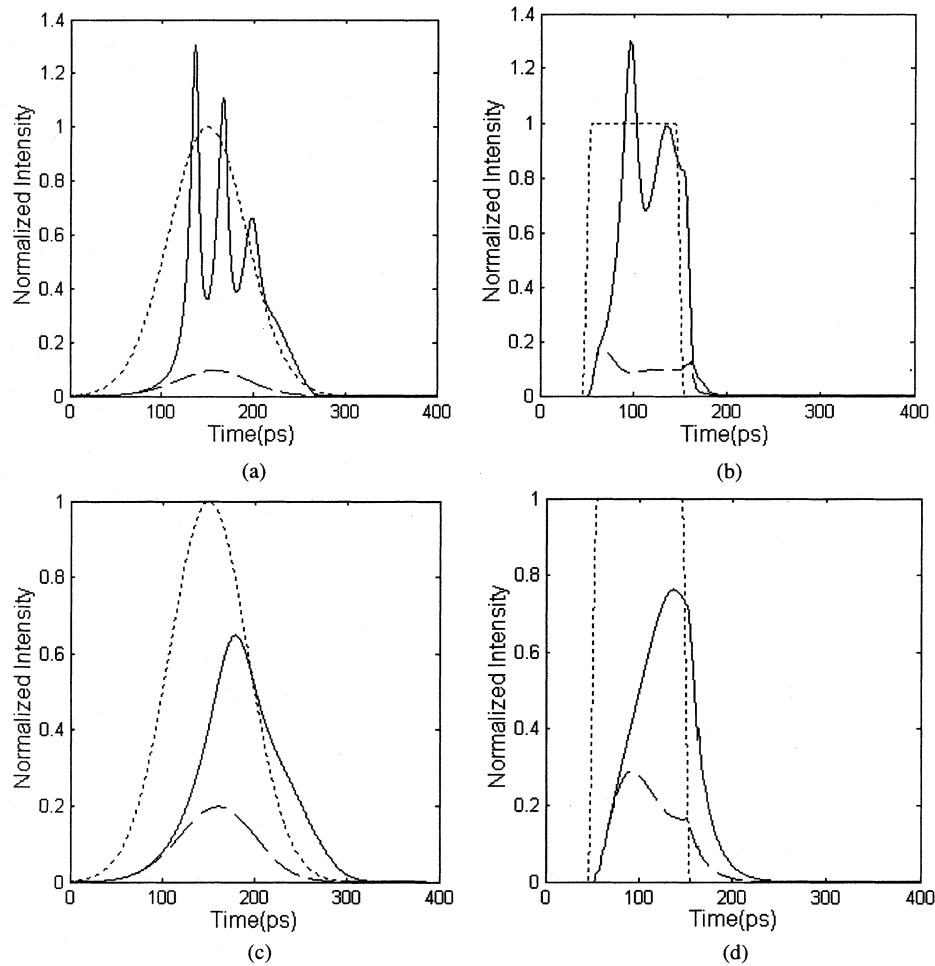


Fig. 12. Transmitted pulse shapes in the on (solid) and off (dashed) states for square- and Gaussian-shape 100-ps input pulses (dotted) in the case of a uniform FBG (top row) and a phase-shifted FBG bottom row.

REFERENCES

- [1] R. Kashyap, *Fiber Bragg Gratings*. San Diego, CA: Academic, 1999.
- [2] H. G. Winful, J. H. Marburger, and E. Garmire, "Theory of bistability in nonlinear distributed feedback structures," *Appl. Phys. Lett.*, vol. 35, no. 5, pp. 379–381, 1979.
- [3] W. Chen and D. L. Mills, "Optical response of nonlinear multilayer structures: Bilayers and superlattices," *Phys. Rev. B*, vol. 36, no. 12, pp. 6269–6278, 1987.
- [4] G. P. Agrawal and S. Radic, "Phase-shifted fiber Bragg gratings and their applications for wavelength demultiplexing," *IEEE Photon. Technol. Lett.*, vol. 6, pp. 995–997, Aug. 1994.
- [5] S. Radic, N. George, and G. P. Agrawal, "Theory of low-threshold optical switching in nonlinear phase-shifted periodic structures," *J. Opt. Soc. Amer. B*, vol. 12, no. 4, pp. 671–680, 1995.
- [6] S. Wabnitz, "Pulse self-switching in optical-fiber Bragg gratings," *Opt. Commun.*, vol. 114, pp. 170–180, 1995.
- [7] U. Mohideen, R. E. Slusher, V. Mizrahi, T. Erdogan, J. E. Sipe, M. Gonokami, P. J. Lemaire, C. M. de Sterke, and N. G. R. Broderick, "Gap soliton propagation in optical fiber gratings," *Opt. Lett.*, vol. 20, no. 16, pp. 1674–1676, 1995.
- [8] J. Liu, C. Liao, S. Liu, and W. Xu, "The dynamics of direction-dependent switching in nonlinear chirped gratings," *Opt. Commun.*, vol. 130, pp. 295–301, 1996.
- [9] B. J. Eggleton, R. E. Slusher, J. B. Judkins, J. B. Stark, and A. M. Vengsarkar, "All-optical switching in long-period fiber gratings," *Opt. Lett.*, vol. 22, no. 12, pp. 883–885, 1997.
- [10] E. Taverner, N. G. R. Broderick, D. J. Richardson, R. I. Laming, and M. Ibsen, "Nonlinear self-switching and multiple gap-soliton formation in a fiber Bragg grating," *Opt. Lett.*, vol. 23, no. 5, pp. 328–330, 1998.
- [11] N. G. R. Broderick, "Bistable switching in nonlinear Bragg gratings," *Opt. Commun.*, vol. 148, pp. 90–94, 1998.
- [12] N. G. R. Broderick, D. J. Richardson, and M. Ibsen, "Nonlinear switching in a 20-cm-long fiber Bragg grating," *Opt. Lett.*, vol. 25, no. 8, pp. 536–538, 2000.
- [13] A. Melloni, M. Chinello, and M. Martinelli, "All-optical switching in phase-shifted fiber Bragg gratings," *IEEE Photon. Technol. Lett.*, vol. 12, pp. 42–44, Jan. 2000.
- [14] V. E. Perlin and H. G. Winful, "Nonlinear pulse switching using long-period fiber gratings," *J. Lightwave Technol.*, vol. 18, pp. 329–333, Mar. 2000.
- [15] —, "Nonlinear pulse switching using cross-phase modulation and fiber Bragg gratings," *IEEE Photon. Technol. Lett.*, vol. 13, pp. 960–962, Sept. 2001.
- [16] G. W. Chern, J. F. Chang, and L. A. Wang, "Modeling of nonlinear pulse propagation in periodic and quasiperiodic binary long-period fiber gratings," *J. Opt. Soc. Amer. B*, vol. 19, no. 7, pp. 1497–1508, 2002.
- [17] D. Pelinovsky and E. H. Sargent, "Stable all-optical limiting in nonlinear periodic structures. II. Computations," *J. Opt. Soc. Amer. B*, vol. 19, no. 8, pp. 1873–1889, 2002.
- [18] S. H. Jeong, H. C. Kim, T. Mizumoto, J. Wiedmann, S. Arai, M. Takehana, and Y. Nakano, "Polarization-independent all-optical switching in a nonlinear GaInAsP-InP high-mesa waveguide with a vertically etched Bragg reflector," *IEEE J. Quantum Electron.*, vol. 38, pp. 706–715, July 2002.

- [19] B. J. Eggleton, R. E. Slusher, C. M. de Sterke, P. A. Krug, and J. E. Sipe, "Bragg grating solitons," *Phys. Rev. Lett.*, vol. 76, no. 10, pp. 1627–1630, 1996.
- [20] B. J. Eggleton, C. M. de Sterke, and R. E. Slusher, "Nonlinear propagation in superstructure Bragg gratings," *Opt. Lett.*, vol. 21, no. 16, pp. 1223–1225, 1996.
- [21] B. J. Eggleton and C. M. de Sterke, "Nonlinear pulse propagation in Bragg grating," *J. Opt. Soc. Amer. B*, vol. 14, no. 11, pp. 2980–2993, 1997.
- [22] A. B. Aceves and S. Wabnitz, "Self-induced transparency solitons in nonlinear refractive periodic media," *Phys. Lett. A*, vol. 141, no. 1, pp. 37–42, 1989.
- [23] R. E. Slusher, B. J. Eggleton, and T. A. Strasser, "Nonlinear pulse reflections from chirped fiber gratings," *Opt. Exp.*, vol. 3, no. 11, pp. 465–475, 1998.
- [24] C. M. de Sterke and J. E. Sipe, "Gap soliton," in *Progress in Optics*, E. Wolf, Ed. Amsterdam, The Netherlands: Elsevier, 1994, vol. 33.
- [25] C. M. de Sterke, K. R. Jackson, and B. D. Robert, "Nonlinear coupled-mode equations on a finite interval: A numerical procedure," *J. Opt. Soc. Amer. B.*, vol. 8, no. 2, pp. 403–412, 1991.



Hojoon Lee (S'84–M'89) was born in Seoul, Korea. He received the B.S., M.S., and Ph.D. degrees from the Department of Electronic Engineering, Sungkyunkwan University, Seoul, Korea, in 1978, 1980, and 1986, respectively.

In 1980, he joined the Korea Military Academy, Seoul, Korea, for three years, where he became a full-time Instructor in the Department of Electronic Engineering. In 1987, he joined the Department of Information and Communication Engineering, Hoseo University, Asan, Korea, where he is currently a Professor of Optical Communications. He was a Postdoctoral Researcher at the Department of Electrical Engineering, Stanford University, Stanford, CA, during 1991 and 1992 and a Visiting Professor at the Institute of Optics, University of Rochester, Rochester, NY, during 2002 and 2003. He has authored or coauthored more than 100 journal and conference papers and has several patents. His research interests include work on optical fiber communications, optical fiber sensor systems, fiber Bragg grating fabrication, and nonlinear pulse propagation in fiber gratings.



Govind P. Agrawal (M'83–SM'86–F'96) received the B.S. degree from the University of Lucknow, Lucknow, India, in 1969 and the M.S. and Ph.D. degrees from the Indian Institute of Technology, New Delhi, in 1971 and 1974, respectively.

After holding positions at the Ecole Polytechnique, France, the City University of New York, and AT&T Bell Laboratories, Murray Hill, NJ, in 1989 he joined the faculty of the Institute of Optics, University of Rochester, Rochester, NY, where he is a Professor of Optics. His research interests focus

on quantum electronics, nonlinear optics, and laser physics. In particular, he has contributed significantly to the fields of semiconductor lasers, nonlinear fiber optics, and optical communications. He is the author or coauthor of more than 300 research papers, several book chapters and review articles, and four books, *Semiconductor Lasers* (Norwell, MA: Kluwer, 1993), *Fiber-Optic Communication Systems* (New York: Wiley, 2002), *Nonlinear Fiber Optics* (New York: Academic, 2001), and *Applications of Nonlinear Fiber Optics* (New York: Academic, 2001). He has also edited two books, *Contemporary Nonlinear Optics* (New York: Academic, 1992) and *Semiconductor Lasers: Past, Present and Future* (New York: AIP, 1995).

Dr. Agrawal was the Program Co-Chair in 1999 and the General Co-Chair in 2001 for the Quantum Electronics and Laser Science Conference. He also chaired a program subcommittee in 2001 for the Nonlinear Guided Waves and their Applications conference. He is a Fellow of the Optical Society of America (OSA).